Investigations into the use of two frequency excitation to accurately determine bubble sizes

A.D. Phelps and T.G. Leighton
Institute of Sound and Vibration Research, University of Southampton, Southampton SO9 5NH

Abstract.
The nonlinear response of bubbles excited at their resonance provides a useful method for sizing them acoustically. Tests have been done previously using two frequencies incident on the bubble - one high fixed imaging frequency and another lower frequency that is adjusted to match the resonant frequency of the bubble. The nonlinear coupling gives rise to sum-and-difference terms, corresponding to the bubble's resonance and to harmonics, subharmonics and ultraharmonics of this resonance. From these the bubble radius can be determined. This paper gives details of investigations into the suitability of this method to actively size bubbles of unknown radius and distribution, and discusses its accuracy and limitations, and the potential for construction of an automated high-resolution time-averaged acoustic bubble sizer.

1 Introduction

The appearance of bubbles in fluid media is an important phenomenon, and a knowledge of their size and number has been used to investigate effects such as decompression sickness [1, 2] contrast echocardiography [3], pressure fluctuation measurements [4] and monitoring the coolant in nuclear reactors [5]. Of increasing interest are studies into oceanic bubbles, which have been shown to be important in understanding and quantifying the gas flux between the atmosphere and the oceans [6, 7].

Bubble measurement lends itself towards the use of acoustics - bubbles have a very high acoustic cross section and can scatter sound very effectively. For low amplitude excitation by a sound field, the bubble wall moves in an approximately linear manner, and the pulsation can be described as a lightly damped single degree of freedom system. As such, it possesses a well-defined acoustic resonance of frequency:

$$\nu_r = \left(\frac{1}{2\pi R_0}\right)\left(\frac{3\kappa P_0}{\rho}\right)^{\frac{1}{2}} \tag{1}$$

where R_0 is the equilibrium bubble radius, κ is the polytropic index of the gas inside the bubble, P_0 is the hydrostatic pressure and ρ is the density of the fluid medium. This was first derived by Minneart [8], who assumed that surface tension and viscosity terms are negligible, and that the bubble wall undergoes simple harmonic motion. For air bubbles in water at atmospheric pressure, equation (1) reduces to:

$$\nu_r R_0 \approx 3\text{Hz m} \tag{2}$$

J. R. Blake et al. (eds.), Bubble Dynamics and Interface Phenomena, 475–484.

Various different acoustical methods have been proposed to make use of this strong scattering property. These include detection of linear backscatter from a bubble insonated at its resonant frequency [9], and by Doppler methods [10]. Both these methods are limited [11]. Linear backscattering is unable to distinguish between a large bubble off resonance and a small bubble at resonance, and using the Doppler technique a larger bubble and a cluster of smaller bubbles can give the same echo. More successful methods have utilised the nonlinear response of bubbles at resonance. An asymmetry is introduced into the motion of a bubble wall at higher amplitude because, for example, it can potentially expand without limit, but only contract to a point as its radius tends to zero. This behaviour manifests itself in the form of oscillations whose frequencies are harmonics of the resonant driving sound field. The second harmonic generation has been used to size bubbles [12], but although it can unambiguously distinguish between bubbles of different sizes, it has very poor spatial resolution, and these frequencies can arise in the absence of bubbles through harmonics produced by transducers, power amplifiers, etc. and through nonlinear propagation.

One technique examined in this paper was introduced by Newhouse and Shankar [13], and relies on examining the nonlinear coupling of two sound fields incident on the bubble. If the bubble is insonated with two frequencies, one a high fixed frequency ω_i (called the *imaging* frequency), and another lower frequency ω_p which is tuned to the resonant frequency of the bubble (called the *pump* frequency), the quadratic term in the nonlinear response will give rise to frequencies at $\omega_i + \omega_p$ and $\omega_i - \omega_p$. Shankar *et al.* [11] took the appearance of these sum-and-difference terms to mean that their pump frequency ω_p equalled the bubble resonant frequency, and they used this value to calculate the bubble size.

However, recent work [15, 14] has shown that the other frequencies stimulated by the nonlinear motion of the bubble wall at resonance, the most prominent of which is a *subharmonic* at $\omega_p/2$, will similarly undergo sum-and-difference coupling with the imaging frequency, and give rise to emissions at $\omega_i \pm \omega_p/2$. These have been shown to be much more accurate indicators of the bubble resonant frequency [14]. This is because this nonlinear response is of a higher order than the fundamental sum-and-difference scattering, and therefore falls off much faster as the bubble is insonated away from resonance, an effect which may be associated with details of the damping [14].

This text reports on the findings of investigations into the fundamental and subharmonic sum-and-difference signals emitted by single bubbles at resonance in an exercise to determine the methodology which would be appropriate for a bubble sizer which would utilise these principles. It examines the resonant response of both the fundamental and the subharmonic sum-and-difference signals, and describes the frequency resolution achievable practically by this method. It also gives details regarding the dependence of the emissions on the amplitude of the pumping signal, and reports on the reproducibility of the tests.

2 Experimental details

The experiment is performed in a 1.8m x 1.2m x 1.2m deep glass reinforced plastic tank which is filled with water to 1 m depth, and is vibration isolated by four 1400 x 300 mm Tico pads spaced equidistantly along its base. The experimental set-up is shown in figure 1. The high frequency imaging signal is provided by a Therasonic 1030 Ultrasound Generator, as manufactured by Electro-Medical Supplies. This provides a continuous tone just above 1 MHz. The low frequency projector is a Gearing and Watson UW60 moving coil underwater loudspeaker, which has a frequency response flat to within $\pm$ 5 dB over the range 500 Hz - 10 kHz. The high frequency receiver is an unfocused Panametrics V302 immersion transducer, which has a resonance at 1 MHz and is highly damped to prevent excessive fall-off either side of this peak. These three transducers are sturdy and remote, making minimally invasive oceanic measurements a possibility. They are all clamped onto a rigid 205 mm x 140 mm x 400 mm high stainless steel cage to maintain their relative alignment from one test to the next, and the whole cage is then rigidly suspended from a stainless steel bar fixed across the width of the tank. This bar is isolated from the tank by foam inserts around its side clamps. The signal to the low frequency projector is driven by a Bruel and Kjaer type 2713A power amplifier, and the returned signal from the receiver transducer is conditioned by a Diagnostic Sonar 5670 battery powered preamplifier. Both projection and detection systems were checked to ensure they introduced no harmonic distortion at the frequency locations of interest.

The relative alignment of the transducers in the cage is such that the low frequency projector and the high frequency receiver face each other with a shared axis of rotation. This is to facilitate the eventual calculation of the volume of water over which the transducers act, so an estimate of gas content per unit volume can be achieved. The Therasonic imaging projector is set perpendicular to the other two transducers to allow the whole area of fluid between them to be insonated. The three transducers are set in the same horizontal plane.

A single bubble is employed to characterise the system, since it is important to ensure that this technique, unlike others currently in operation, is not capable of erroneous triggering. The bubble is attached to a thin wire coated sparingly in petroleum jelly. This wire is fixed horizontally 4 cm from the front face of the Gearing and Watson transducer by means of clamps on the projector and the cage. The wire is fixed horizontally to prevent bubbles being displaced by buoyant forces which could move the bubble from the transducers' focal area during the experiment.

The signal processing and automation was controlled by a specialist custom-designed data acquisition unit. The purpose of this unit is to co-ordinate the pump frequency output and high frequency input signals, and to provide a rapid high frequency resolution FFT of the data. The system works by reading a file from the P.C. which specifies the input frequencies for the pump signal generator, a

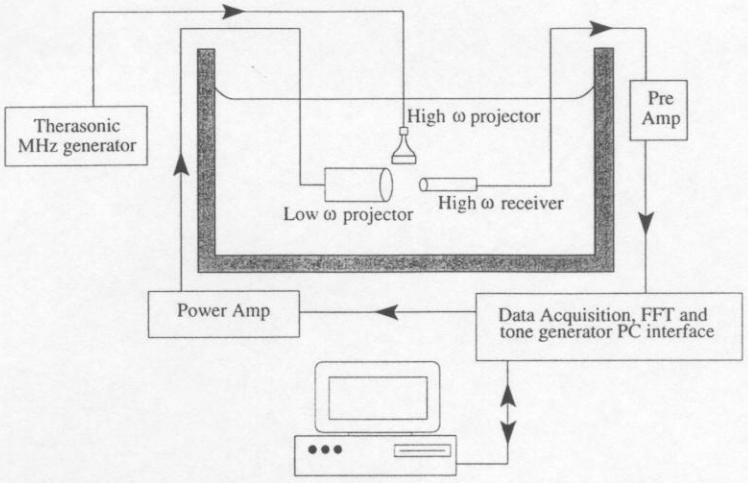

Fig. 1. The equipment and experimental arrangement used in the tests. The three transducers are drawn out of the horizontal for clarity.

corresponding amplitude multiplier to allow correction for the frequency response of the projector/amplifier, and the final frequency window of interest (this is obviously set around the Therasonic signal generator frequency). The unit then sends out a signal to the projector at the first frequency value, and simultaneously takes in data from the high frequency receiver. This data is then decimated and heterodyned, and a 8192 point FFT is taken which spans the frequency window specified in the P.C. file, with each frequency bin 5 Hz apart. This is then saved onto a RAM disk set up on the P.C., and the unit repeats the tests using the second input frequency, and so on. This allows the bubble's dependence on two important parameters to be investigated, namely the pumping signal amplitude, and the frequency step size between successive projector outputs.

3 Results

The output returned from a single run of the tests described earlier is given in figure 2 as a mesh plot. The data were collected from a bubble insonated at 95 Pa, and the pumping frequency was stepped through its resonance in 25 Hz intervals. For all the tests presented here the pumping frequency was decremented through the bubble resonance, as incrementing the signal experimentally gave a second local maximum in the subharmonic response when the bubble was insonated just below resonance. The plot shows the measured response in a narrow frequency window (1,132,900 Hz to 1,138,600 Hz) over twenty different pumping frequencies, going from 1825 Hz to 2300 Hz. The main ridge, which is constant over the twenty tests, is the imaging signal from the Therasonic frequency generator at 1,134,700 Hz. The Therasonic generates spurious side lobes which are clearly visible either side of its centre peak, and these are also evident around the sum-and-difference

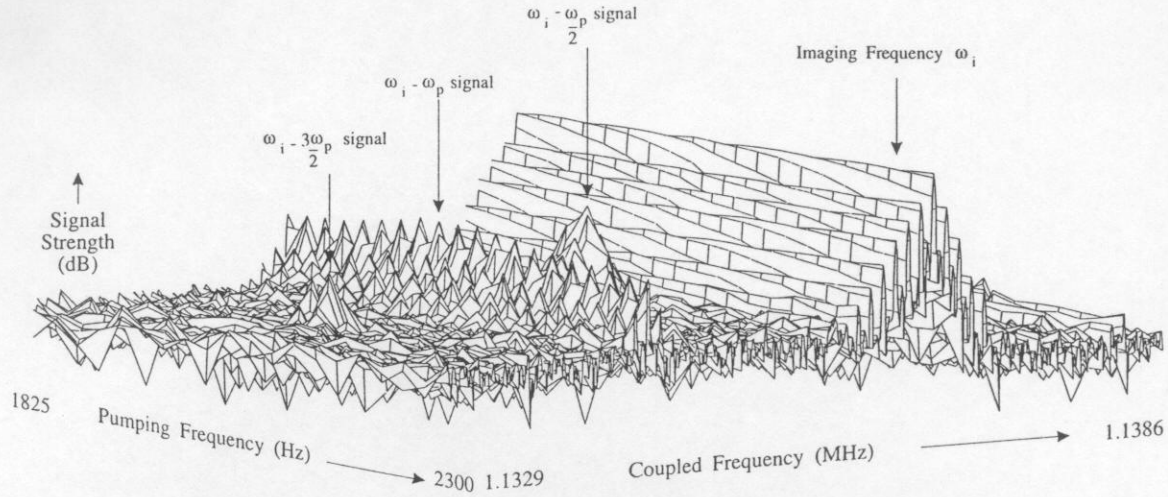

Fig. 2. Mesh plot of returned signal strength through a bubble's resonance. The bubble was insonated at 95 Pa and the pumping frequency was stepped in 25 Hz intervals.

signals. To the left of the imaging signal on figure 2 is a broken ridge which similarly is present over all twenty pumping signals - this is the coupled response corresponding to $\omega_i - \omega_p$. Between the two bands is a single peak which occurs at a pumping frequency of 2050 Hz. This is due to the subharmonic emission from the bubble, and is located at $\omega_i - \omega_p/2$. An ultraharmonic signal is also visible over a very localised pumping frequency span located at $\omega_i - 3\omega_p/2$, although it is not as prominent as the subharmonic signal. These results are also displayed on figure 3, which shows the height of the fundamental difference signal at $\omega_i - \omega_p$ and the subharmonic difference signal at $\omega_i - \omega_p/2$ over the pumping frequency range for the same data. Also shown on the plot are the signals at both the fundamental and the subharmonic difference frequencies in the absence of a bubble. The plot shows that the subharmonic coupled emission is considerably narrower than the fundamental signal, and stands about 25 dB above the background noise level. It is also evident that even in the absence of a bubble, the signal at the fundamental difference location is still 10 dB above the noise floor, suggesting that some coupling still exists. The y-axis from both plots shows signal strength in dB with a common but arbitrary reference value. This is because the level of the signal picked up from the receiver transducer is directly proportional to the level output from the imaging projector, and therefore only relative comparisons are important.

The second set of tests were run in an attempt to investigate the dependence of the output response on the level of the pumping signal. Figure 4 shows the results of one such test. The bubble was insonated through its resonance at 40 discrete pumping frequencies in 5 Hz steps, and each run the pumping signal's strength was increased by 2.5 Pa. The plot shows four such responses, which correspond to 60 Pa, 70 Pa, 75 Pa and 85 Pa. The response at 60 Pa shows that no subharmonic is present in the noise, and therefore that a definite excitation threshold exists.

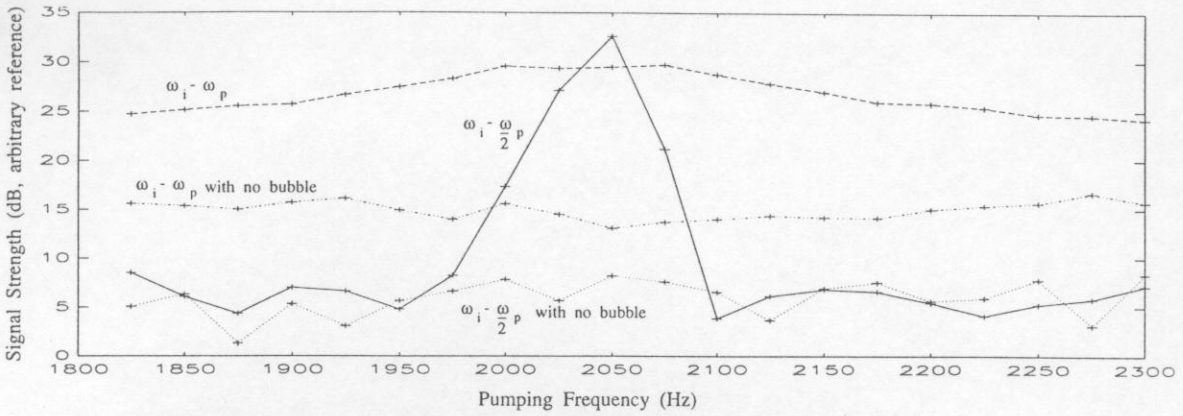

Fig. 3. Plot of the height of the fundamental difference signal (dashed line) and the subharmonic difference signal (unbroken line) through a bubble's resonance, and the signals in the absence of a bubble at the same fundamental location (dash-dot line) and subharmonic location (dotted line). The bubble was insonated at 95 Pa and the pumping frequency was stepped in 25 Hz intervals.

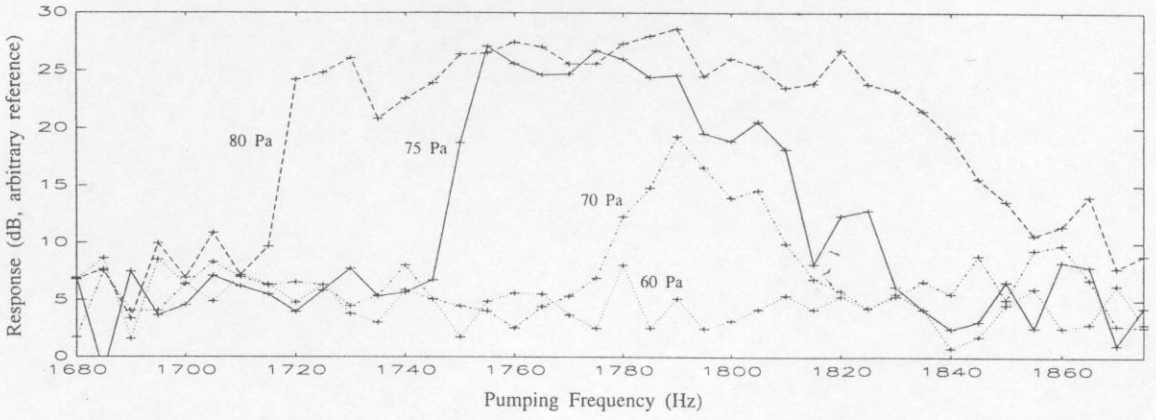

Fig. 4. Plot showing the variation in sum-and-difference subharmonic height through resonance as the strength of the pumping frequency is altered. The frequency step size is 5 Hz, and the lines correspond to pressure amplitudes of : 60 Pa (dotted), 70 Pa (dash-dot), 75 Pa (unbroken) and 85 Pa (dashed).

This threshold has been demonstrated to be higher than that for the fundamental sum-and-difference signal [15]. The subharmonic response corresponding to an insonation at 70 Pa shows a peak in the signal with an unambiguous maximum - this can be used to very accurately determine the resonant frequency of the bubble to within ± 2.5 Hz. However, when the bubble is insonated at 75 Pa and above the response becomes overdriven, and there is an increase in the frequency range of the pumping signal over which a subharmonic can be exacted. Therefore the exact location of the bubble's resonant frequency is less obvious. Again, the y-axis shows the response in decibels with a common, but unfixed reference value.

The final tests reported are shown on figure 5. These involve an investigation into the reproducibility from one test to the next. A bubble which was resonant

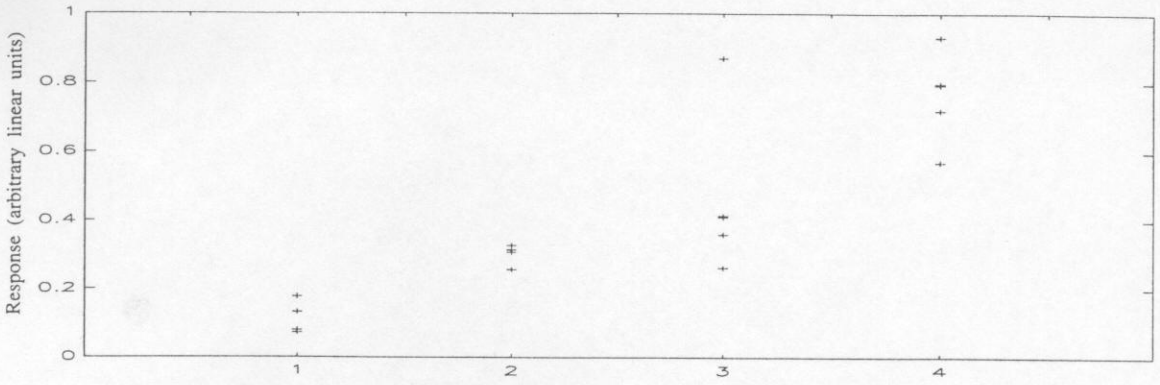

Fig. 5. Reproducability tests for a bubble driven at the threshold of subharmonic excitation (70 Pa) and again slightly overdriven (80 Pa). The graph shows the maximum values over five repeated tests of: column 1 - excitation threshold subharmonic heights, column 2 - excitation threshold fundamental heights, column 3 - slightly overdriven subharmonic heights and column 4 - slightly overdriven fundamental heights. The y axis has been scaled to between 0 and 1 for ease of representation.

at approximately 2200 Hz was insonated at 70 Pa and again at 80 Pa, which from the results given in figure 4 represent being driven at the threshold of subharmonic excitation and well into the overdriven region respectively. The bubbles were again stepped through in 5 Hz steps, and each run was exactly repeated five times. The peak values from both the subharmonic $(\omega_i + \omega_p/2)$ and the fundamental $(\omega_i + \omega_p)$ responses over each run were then calculated. Figure 5 shows these results as the 70 Pa subharmonic heights in column 1, the 70 Pa fundamental heights in column 2, the 80 Pa subharmonic heights in column 3 and the 80 Pa fundamental heights in column 4. The response has been scaled to between 0 and 1 for ease of representation, as again the absolute values are not important. The results show a spread of 3.9 dB for the excitation threshold subharmonic and 1.1 dB for the fundamental, and a spread of 5.2 dB for the overdriven subharmonic but only 2.1 dB for its corresponding fundamental.

4 Discussion

As expected, the scattered signal from the subharmonic sum-and-difference response gives a sharper and therefore more accurate estimate of the location of the bubble resonance. It is also apparent that while the subharmonic emission rapidly drops off to the noise floor when the bubble is insonated off resonance, the fundamental sum-and-difference signal falls at a considerably slower rate, demonstrating that the $\omega_i \pm \omega_p$ signal can still be exacted from a bubble far from its resonance. The tests performed in the absence of a bubble demonstrate that the signal at the fundamental sum-and-difference location is still 10 dB above the noise floor, and that therefore some nonlinear coupling between the two interrogating sound fields

is still occurring. Hence, simply finding a signal at a $\omega_i \pm \omega_p$ location is insufficient to indicate the presence of a bubble. These emissions result from direct action of the low frequency projector on the receiver transducer, and can arise through other coupling effects. The subharmonic, however, is created by the bubble's nonlinear response to the incident pumping signal, which in turn couples with the imaging sound field, and is hence an unambiguous indicator of a bubble's presence.

The use of this method for automated bubble sizing and counting presents some interesting questions. It is clear (figure 4) that a very definite amplitude threshold exists below which no signal at $\omega_i \pm \omega_p/2$ is detected. Above this threshold the subharmonic signal rapidly spreads out along the frequency axis such that a subharmonic response can be exacted from a bubble when the pumping frequency is further and further away from the resonant frequency. Thus a compromise needs to be arrived at between the amplitude of excitation, and the step size which the pumping signal decreases by each time the data is collected. As the step size is decreased and the frequency resolution of the scan improves, the insonation amplitude must also be reduced to preserve the definition of the peak. By slightly 'under sampling' the bubble population a trade-off will exist where one bubble will give rise to a single, or at least unambiguous, subharmonic peak while the amplitude of the input signal can be set slightly higher than the threshold value for that bubble size, and hence be certain that a strong subharmonic signal will be returned.

The tests performed to investigate the reproducibility of the method show the importance of setting the input signal strength above the subharmonic threshold. Because the subharmonic emission is several bifurcations towards chaos, it is fairly non-deterministic and the strength of the returned signal is unpredictable. However, the tests show that the level of the fundamental signal at the bubble's resonance is considerably easier to anticipate. This gives two interesting options open when sizing a bubble cloud. If the height of the subharmonic signal is unpredictable when a bubble is being insonated at resonance, then two bubbles of the same size will be indistinguishable from one alone. The problem could be solved by stepping through the population with a very small frequency decrement and an amplitude function which exactly matches the subharmonic threshold, and to then to assume that every peak represents a bubble. This may be impractical due to the difficulty in implementing such a control over the pumping signal's amplitude at the bubble. Alternatively, the step size could be increased, allowing more flexibility in the amplitude of the interrogating signal. This way the subharmonic signal could be used to locate the bubbles, and the height of the fundamental signal used to count them. The level of the $\omega_i \pm \omega_p$ signal due to the nonlinear mixing by a bubble stands around 10-15 dB above the direct coupled level, and so the amplitude of the returned signal would be an accurate measure of the number of bubbles. This would greatly speed up a sweep over a large frequency span - recent experiments in the oceans [16] suggest that to be sure of measuring 95% of the air volume at 0.1m depth contained in bubbles a sweep must be able to detect

bubbles down to $20\mu m$ in radius (i.e. 150,000 Hz pump frequency from equation (2).)

5 Conclusions

When a bubble is insonated at two frequencies, an audio frequency pump signal which is tuned to the resonant frequency of the bubble and a high frequency imaging signal, the nonlinear coupling of the sound fields presents a method of locating and sizing them. These results give further indication that locating the resonant frequency by the $\omega_i \pm \omega_p/2$ subharmonic stimulation at resonance is a more accurate indicator than by simply looking for the signal at $\omega_i \pm \omega_p$. Indeed, this has been shown to be present even in the absence of a bubble from a straight coupling of the two sound fields. The possibility of an automated bubble sizer is not impractical, but would require a careful balance involving the interval between consecutive pumping tones and the amplitude of the signals. Provided that the bubbles are not insonated too far above their subharmonic amplitude threshold, it may be possible to use the narrow subharmonic response to locate the bubble's resonant frequency accurately, and the height of the $\omega_i \pm \omega_p$ signal to count the number occurring in that frequency band.

Acknowledgements

The authors wish to thank the Natural Environment Research Council who have funded the project, reference SIDAL 00670, and Mr. A. Hardwick for useful discussions.

References

1. Belcher, E.O. Quantification of bubbles formed in animals and man during decompression *IEEE Trans Biomed Eng* (1980) **27** 330-338
2. Kisman, H. Spectral analysis of Doppler ultrasonic decompression data *Ultrasonics* (1977) **15** 105-110
3. Tickner, E.G. Precision microbubbles for right side intercardiac pressure and flow measurements, in: *Contrast Echocardiography* (Eds. Meltzer, R.S. and Roeland, J.) Nijhoff, London, UK (1982)
4. Hulshof, H.J.M. and Schurink, F. Continuous ultrasonic waves to detect steam bubbles in water under high pressure *Kema Scientific and Technical Reports* (1985) **3** 61-69
5. Watkins, R.D., Barrett, L.M. and McKnight, J.A. Ultrasonic waveguide for use in the sodium coolant of fast reactors *Nucl Energy* (1988) **27** 85-89
6. Thorpe, S.A. On the clouds of bubbles formed by breaking wind waves in deep water, and their role in air-sea gas transfer *Phil Trans R. Soc Lond* (1982) **304** 155-210
7. Woolf, D.K. and Thorpe, S.A. Bubbles and the air-sea exchange of gases in near saturation conditions *Journal of Marine Research* (1991) **49** 435-466
8. Minnaert, M. On musical air-bubbles and sounds of running water *Phil Mag* (1933) **16** 235-248
9. Fairbank, W.M. and Scully, M.O. A new non-invasive technique for cardiac pressure measurement: resonant scattering of ultrasound from bubbles *IEEE Trans Biomed Eng* (1977) **24** 107-110

10. Nishi, R.Y. Ultrasonic detection of bubbles with Doppler flow transducers *Ultrasonics* (1972) **10** 173-179
11. Shankar, P.M., Chapelon, J.Y. and Newhouse, V.L. Fluid pressure measurement using bubbles insonified by two frequencies *Ultrasonics* (1986) **24** 333-336
12. Miller, D.L. Ultrasonic detection of resonant cavitation bubbles in a flow tube by their second-harmonic emissions *Ultrasonics* (1981) **19** 217-224
13. Newhouse, V.L. and Shankar, P.M. Bubble size measurement using the nonlinear mixing of two frequencies *JASA* (1984) **75** 1473-1477
14. Leighton, T.G., Lingard, R.J., Walton, A.J. and Field, J.E. Acoustic bubble sizing by combination of subharmonic emissions with imaging frequency *Ultrasonics* (1991) **29** 319-323
15. Hardwick, A.J., Leighton, T.G., Walton, A.J. and Field, J.E. Acoustic bubble sizing through nonlinear combinations involving parametric excitations *European Conf on Underwater Acoustics* (Ed. M. Weydert) publ Elsevier Applied Science (1992) 153-156
16. Farmer, D.M. and Vagle, S. Waveguide propagation of ambient sound in the ocean surface bubble layer *JASA* (1989) **86** 1897-1907